Finite Element Analysis Relating Shape, Material Properties, and Dimensions of Taenioglossan Radular Teeth with Trophic Specialisations in Paludomidae (Gastropoda)

Wencke Krings (wencke.krings@uni-hamburg.de)
Universität Hamburg
Jordi Marcé-Nogué
Rovira i Virgili University
Stanislav N. Gorb
Kiel University

Research Article

Keywords: Functional morphology, FEA, mechanical properties, ecology, Lake Tanganyika

Posted Date: August 26th, 2021

DOI: https://doi.org/10.21203/rs.3.rs-835609/v1

Version of Record: A version of this preprint was published at Scientific Reports on November 23rd, 2021. See the published version at https://doi.org/10.1038/s41598-021-02102-8.

Abstract

The radula, a chitinous membrane with embedded tooth rows, is the molluscan autapomorphy for feeding. The morphologies, arrangements and mechanical properties of teeth can vary between taxa, which is usually interpreted as adaptation to food. In previous studies, we proposed about trophic and other functional specialisations in taenioglossan radulae from species of African paludomid gastropods. These were based on the analysis of shape, material properties, force-resistance, and the mechanical behaviour of teeth, when interacting with an obstacle, which was previously simulated for one species (*Spekia*) by the finite-element-analysis (FEA) and, for more species, observed in experiments. In the here presented work, we test the previous hypotheses by applying the FEA on 3D modelled radulae, with incorporated material properties, from three additional paludomid species. These species forage either on algae attached to rocks (*Lavigeria*), covering sand (*Cleopatra*), or attached to plant surface and covering sand (*Bridouxia*). Since the analysed radulae vary greatly in their size between species, we additionally aimed at relating the simulated stress and strain distributions with the tooth sizes by altering the force/volume. For this purpose, we also included *Spekia* again in the present study. Our FEA results show that smaller radulae are more affected by stress and strain than larger ones, when each tooth is loaded with the same force. However, the results are not fully in congruence with results from the previous breaking stress experiments, indicating that besides the parameter size, more mechanisms leading to reduced stress/strain must be present in radulae.

1. Introduction

1.1. The molluscan autapomorphy for feeding, the radula

The radula is the molluscan autapomorphy for food gathering and processing. It consists of a chitinous membrane with embedded rows of teeth, which interact with the preferred food and the substrate the food is attached to (feeding substrate). Underlain odontophoral cartilages mechanically support the thin radula. Buccal mass muscles move it during foraging, resulting in shearing, cutting, and gathering actions [1–6]. Teeth usually have contact with the ingesta at their tooth cusps, which can be situated on elongated styli; these are connected to the radular membrane by their tooth bases (see Fig. 1). The tight interaction of teeth with the ingesta leads to some tooth wear [e.g. 8–13], but the radula is constantly secreted and maturated by overlain epithelia in its posterior parts, the radular sack and formation zone [e.g. 14–19]. Then, mature teeth enter the radular anterior part, the working zone, where they are in use. Afterwards teeth eventually break loose in the degenerative zone and are probably digested.

1.2. Functional and trophic specialisations of radular teeth

As the radula is the main structure, used for the acquisition of food, and the teeth represent the interface between organism and environment, the organ can show (a) functional specialisations of tooth types (loosening of food items, collecting particles, reinforcement of the radula, etc.) and (b) trophic adaptations. Both types of specialisations are related to one another and can be reflected by radular morphology and structure [e.g. 13,20–41] and by tooth material properties (i.e. hardness and Young's modulus) [e.g. 5,10,40,42–51]. Gradients in these properties can contribute to the functionality of a structure by e.g. distributing stress, enabling deformation or the resistance to structural failure [e.g. 52–57] and are present in teeth of chitons, limpets [43, 45, 58], and paludomid gastropods [48–49, 51].

1.3. Model system African Paludomidae

The Paludomidae from Lake Tanganyika and surrounding water bodies are representatives of a species flock, that is potentially the result of an adaptive radiation accompanied by trophic specialisation [for hypotheses on paludomid evolution see e.g. 40,50,59–68]. They possess taenioglossan radulae (seven teeth per row: one central, two laterals, two inner and two outer marginals) that show a great interspecific morphological diversity [see e.g. 40,50,68–69]. The species of the flock, that have been in focus of previous studies on trophic specialisation, are substrate-specific and feed algae either from soft (sandy or muddy substrate), mixed (plant surface, sand, mud, and/or rock), or solid substrate (rocks) [40, 50–51]. Some tooth shapes [40, 50] and the size and thickness of the tooth's attachment with the underlain radular membrane [41] were previously analysed and identified as adaptations to the preferred feeding substrate. Additionally, some taxa (all mixed and solid substrate feeders; e.g. *Bridouxia*, *Lavigeria*, *Spekia*) exhibit material property gradients along their teeth, with the cusp as the stiffest and hardest part, followed by the stylus, and finally the basis [48, 51]. We additionally detected that soft substrate feeders (e.g. *Cleopatra*) possess teeth with rather homogeneous material properties; thus the existence or absence of large-scaled gradients were previously also identified as adaptations [51].

1.4. Mechanical behaviour of teeth

The mechanical behaviour of structures can be computer-simulated and visualized by the finite-element-analysis (FEA), a software-based virtual method that solves mechanical problems. Here, bodies with defined material properties can be tested under the action of outer forces, resulting in the visualization of the deformation and distribution of stress and strain. This method was previously employed on various biological objects as a very useful approach in ecomorphological analyses of food processing structures [e.g. 70–82].

The FEA on radulae has been previously conducted on the dominant lateral tooth of the docoglossan radulae from polyplacophoran species [8, 58] and gastropod *Patella* [8], on the isodont radula from the gastropod *Euhadra* [83], and on the taenioglossan radula from the gastropod *Spekia* [49]. The past stress and strain simulations, leading to hypotheses on the functional significance of the local material properties (deformation, transmission of stress, reduction of abrasion) and also tooth function, are either based on 2D shape and material property gradients [8], on 3D shape with a homogeneous material [83], or on 3D shape including material property gradients [49, 58]. In our previous FEA approach on the paludomid *Spekia*, we were able to identify the functional relationship between the shape and properties: we tested the properties' effect on the stress and strain distribution by excluding or including gradients in the tooth FEA-model [49]. Hereby we detected that heterogeneous teeth (with gradients in Young's modulus) have a higher capability of bending and transferring forces than homogeneous teeth (without gradients in Young's modulus).

The proposed mechanical behaviour of *Spekia*'s teeth under load has been later subsequently verified in the breaking stress experiments, where shear load was applied to individual tooth cusps of wet and dry radulae with a needle [84]. Here the force, needed to break teeth, and the behaviour of teeth (bending, twisting, and relying on other teeth) could be documented. Tooth failure under wet (native) condition usually occurred at two sites: (a) the long and slender outer teeth (marginal teeth) failed at their softest and most flexible part, at the stylus close to the basis. (B) The short and relatively stiff inner teeth (central and lateral teeth) relied on the adjacent teeth and did not break until the radular membrane ripped off. The cusps as the hardest and stiffest parts were not as prone to failure. These real experiments verified the previous computer based FEA simulations on *S. zonata*, displaying high values of stress in the marginal styli close to the bases, whereas the harder and stiffer marginal tooth cusps, the centrals, and the laterals are almost not affected by the stress under load [49]. Additionally, we discovered by these breaking stress experiments, that significantly higher force was needed to break wet teeth than dry ones. This was due to the interaction between adjacent teeth of the same type: wet teeth were capable of relying on teeth of adjacent rows [84–85], enabled by mechanical property gradients [see also 48,51], morphology [see also 40,49], and their embedment in the radular membrane [see also 41], leading to a higher force resistance due to a 'collective effect'. Several previous hypotheses, proposed after examination of mounted radulae with scanning-electron-microscope (SEM), on the functional significance of the interaction of radular parts resulting in a proper stress distribution [41, 86–91] have been confirmed by our biomechanical experiments. A broader taxon sampling of paludomid gastropods (e.g. *Lavigeria*, *Cleopatra*, *Bridouxia*) in further breaking stress experiments demonstrated, that the degree, to which this 'collective effect' is pronounced, can be directly related to the gastropod's ecology [84–85]: species foraging on solid substrate (e.g. *Lavigeria* and *Spekia*) exhibit central and lateral teeth that can resist relatively high forces due to their capability of relying on one another. Teeth of species foraging on mixed substrate (e.g. *Bridouxia*) can resist to less force, but their centrals and laterals are also capable of bending and gaining support. Species feeding on algae from soft substrate (e.g. *Cleopatra*) possess teeth that could resist to least forces, since they rather failed individually, even though exhibiting very high bending amplitude in the experiment.

Overall, from analysis of morphology [40–41], breaking stress experiments [84–85], material property data [48, 50–51], and from consolidated 3D shape and material properties [49] we were able to identify trophic specialisations to the feeding substrate, but could also propose the terms 'monofunctional radula' and 'multifunctional radula' for paludomid gastropods [51, 85]. A monofunctional radula possesses only teeth that have a high ability to bend and deform and rather collect food particles from the soft substrate. Multifunctional radulae exhibit inner teeth (centrals and laterals) that are stiffer and able to rather loosen food particles from solid or mixed substrate, and outer teeth (marginals), that are flexible and mainly collect the loosened particles.

1.5. Aim of the study

Using our protocol introduced on *Spekia zonata* [49], we here apply FEA on 3D modelled radulae, with incorporated material properties, from three additional paludomid species. They forage either on solid (*Lavigeria*), soft (*Cleopatra*), or mixed substrate (*Bridouxia*) and possess, as proposed, either a multifunctional (*Lavigeria*, *Bridouxia*) or a monofunctional radula (*Cleopatra*). We were able to test our previous hypotheses on functional specialisations of tooth types and trophic specialisations for these species. As the analysed radulae of adult gastropods vary greatly in their size between species (from 120 to 350 µm), we here additionally aimed at relating the stress and strain distributions with the tooth sizes by considering the force per volume. For this purpose, we also included results previously obtained on *Spekia* in the present study. We detected, as expected, that smaller radulae show greater stress and strain in the FEA than larger ones, when each tooth is loaded with the same force. However, the results of the FEA are not fully in congruence with the results from the previous breaking stress experiments [84–85], indicating that more mechanisms in addition to the size, leading to a resistance to stress and strain, must be present in real radulae.

2. Materials And Methods

2.1. Specimens, radular size and 3D models

The 3D models, used here for finite-element-analysis, were already published for visualisation purposes of breaking stress experiments (*Cleopatra*, *Bridouxia*, *Lavigeria*) and for conducting FEA (*Spekia*) [49, 85].

Originally the models (Fig. 2) were created by studying the radulae from adult gastropod specimens (see Fig. 1 for SEM images and 3 for schematic drawings), that had been either collected by Heinz Büscher in Lake Tanganyika at Zambia, Northern Province, Mibwebwe, in 2019 (*Lavigeria grandis* [Smith, 1881]), at Zambia, Northern Providence, Cape Kachese, in 2016 (*Bridouxia grandidieriana* [Bourguignat, 1885]), by Frank Riedel at Burundi and by Heinz Büscher at Zambia, Kalambo Falls Lodge, in 2017 (*Spekia zonata* [Woodward, 1859]), or by Anthony Wilson in Zambia, Lake Mweru, Nchelenge, in 2000 (*Cleopatra johnstoni* Smith, 1893). These gastropods were preserved in 70% EtOH and either inventoried at the Zoological Museum Hamburg (ZMH; *B. grandidieriana*: ZMH 119367/999; *L. grandis*: ZMH 154657/999; *S. zonata*: ZMH 150008/999) or the Museum für Naturkunde Berlin (ZMB; *C. johnstoni* Smith, 1893: ZMB 220.102; *S. zonata*: ZMB 220.144).

To receive models, two adult specimens per species were dissected, radulae were extracted by tweezers, and cleaned following the protocol of Holznagel [92]. Radulae were first mounted on SEM sample holder, air dried, and documented with the SEM Zeiss LEO 1525 (One Zeiss Drive, Thornwood, NY) (Fig. 1). These images of the two radulae were used for determining the mean width of the radular membrane in the working zone, which was later used for scaling the models (see below). Afterwards, radulae were rewetted with 70% EtOH, loosened from the carbon tape, and manually destroyed by tweezers to receive as many individual teeth as possible. Then, teeth were mounted again on SEM holders in different positions and visualized again by SEM. By this procedure, we received images of individual teeth from different perspectives. With the 3D software Maya 2019 (Autodesk, Inc., San Rafael, USA), one model per tooth type was then formed by hand, always comparing the model with the SEM images to receive ideal 3D teeth. This time-consuming protocol was necessary, as we could not receive good models by the µ-CT technique, because tooth structures are too small and of a low contrast. Afterwards, tooth models were first filled, then copied multiple times and some mirrored, to obtain seven teeth per row and overall two tooth rows. Then teeth were assembled and interlocked as observed during breaking stress experiments under load [84–85]. Then, one side of the generated radular model was cut to receive half of a radula. In Maya,

all models were sized (Fig. 4) in accordance with the data obtained from SEM images (Fig. 1). Then, the volume of the two half-rows could be read out in Maya. Finally a box, representing the membrane, was modelled for each species and merged with the teeth. Surface irregularities were repaired using Geomagic Wrap 2017 (3D Systems, Inc., Moerfelden-Walldorf, Germany) and models were converted to CAD file format necessary for ANSYS FEA Package, as done previously [49].

2.2. Young's modulus

The mechanical properties (Young's modulus) of the teeth of species studied were identified in previous studies at the cusps and styli of the lateral and central teeth and on the bases, styli, and cusps of the marginal teeth I and teeth II by nanoindentation [48, 50–51]. To perform these measurements, 30 radulae were extracted from adult specimens (see Table 1), freed from surrounding tissue by tweezers, and air dried. With double-side adhesive tape, one lateral side of each radula (the marginal teeth II) was taped to a glass object slide and surrounded by a small metallic ring. This ring was filled with epoxy (RECKLI EPOXIWST, RECKLI GmbH, Herne, Germany; Young's modulus – 1 GPa) and left to polymerize at room temperature for two days. Then, both object slide and tape were removed and each sample surface was polished and smoothened [for details, see 48,50–51].

Table 1

Summary of the preferred feeding substrate with the references, the previously assigned feedings substrate category (mixed, solid, and soft; from Krings et al., Krings, 2021), and previously determined Young's moduli (GPa) of the distinct tooth parts (with collection number and quantity of analysed specimens, and analysed tooth parts (data from Krings et al., 2019, 2021b, Gorb & Krings, 2021) are provided for each species studied. Geometrical variables of radulae (widt and volume of the model) necessary to determine the nominal force for each species. N = quantity, SD = standard deviation.

Species	Feeding substrate	Reference for feeding substrate	Feeding substrate category	Summary from previous nanoindentation analysis						Measurements for F	
				Collection number	N of analysed specimens	Tooth type	Tooth part	N of analysed teeth	Young's modulus, GPa, mean	Width of radula, µm mean ± SD	Volume, µm³
Bridouxia grandidieriana (Bourguignat, 1885)	Sand Plant surface	[68, 118–119]; personal comment from one collector (Matthias Glaubrecht)	Mixed	ZMH 119367/999	9	Central tooth	Cusp	167	5.8	120 ± 7	1728000
							Stylus		4.7		
						Lateral tooth	Cusp	176	5.6		
							Stylus		4.4		
						Marginal tooth I	Cusp	156	4.4		
							Stylus		3.6		
							Basis		3.4		
						Marginal tooth II	Cusp	141	4.5		
							Stylus		3.4		
							Basis		3.3		
Lavigeria grandis (Smith, 1881)	Rock	[68–69, 120–121]	Solid	ZMB 220.018, ZMH 150020/999	6	Central tooth	Cusp	84	8.1	350 ± 11	4288200
							Stylus		6.8		
						Lateral tooth	Cusp	111	6.5		
							Stylus		5.1		
						Marginal tooth I	Cusp	106	4.6		
							Stylus		3.3		
							Basis		2.4		
						Marginal tooth II	Cusp	102	4.4		
							Stylus		3.4		
							Basis		2.5		
Cleopatra johnstoni Smith, 1893	Sand Mud	Unpublished work, personal comment from one collector (Matthias Glaubrecht)	Soft	ZMB 220.102b	8	Central tooth	Cusp	151	4.7	220 ± 9	1064600
							Stylus		4.6		
						Lateral tooth	Cusp	123	4.6		
							Stylus		4.3		
						Marginal tooth I	Cusp	101	4.6		
							Stylus		4.6		
							Basis		4.5		
						Marginal tooth II	Cusp	143	4.8		
							Stylus		5.1		
							Basis		4.6		
Spekia zonata (Woodward, 1859)	Rock	[61, 68–69, 118–124]; personal comment from collectors (Heinz Büscher and Matthias Glaubrecht)	Solid	ZMB 220.077, ZMB 220.143, ZMH 150008/999	7	Central tooth	Cusp	110	8.1	250 ± 10	1572500
							Stylus		6.7		
						Lateral tooth	Cusp	112	5.8		
							Stylus		5.0		
						Marginal tooth I	Cusp	57	4.9		
							Stylus		4.1		
							Basis		2.2		

Marginal tooth II	Cusp	60	4.6
	Stylus		3.3
	Basis		2.4

Nanoindentation was performed under normal room conditions (relative humidity 28–30%, temperature 22–24°C) with a Nanoindenter SA2 (MTS Nano Instrument, Oak Ridge, TN, USA) equipped with a Berkovich indenter tip. Young's moduli were determined from force-distance curves; each indent and its curve were manually controlled. This method is based on the continuous stiffness measurement technique [93]. First, marginal teeth were measured, then the samples were polished and smoothened again, to measure the lateral teeth. These steps were repeated until all teeth were analysed. We tested the 20 outermost tooth rows under dry condition; centrals and laterals were tested at two localities (stylus and cusp) and the marginal teeth I and marginal teeth II at three localities (basis, stylus, and cusp). Young's moduli of materials were either determined at penetration depths of 480–520 nm (for tooth cusps of *Spekia* and *Lavigeria*), 460–500 nm (for tooth cusps of *Bridouxia* and *Cleopatra*, for styli and bases of *Spekia* and *Lavigeria*), or 440–480 nm (for styli and bases of *Bridouxia* and *Cleopatra*). We thereby detected in *Spekia*, *Lavigeria*, and *Bridouxia* gradients within each tooth, with the cusp as the stiffest part, followed by stylus, and finally basis. In *Cleopatra*, all teeth were rather homogeneous in this property.

In the present study, the mean values of the previously measured Young's moduli (see Table 1) were assigned to the areas of the models, where they were detected (basis, stylus, cusp; see Fig. 3), as it was previously done for *Spekia* [49]. By employing the thermal diffusion method [94] of the FEA package, values were smoothly diffused through the teeth [see also 95]. Due to the low thickness of the membrane and due to the rapid mechanical changes while drying, we were not able to measure the hardness and elasticity of the membrane by nanoindentation. We therefore assigned the smallest Young's modulus value, measured for the species' teeth (following the protocol of [49]), to the membrane of each model (in *Bridouxia*: 3.3 GPa, *Lavigeria*: 2.4 GPa, *Cleopatra*: 4.3 GPa, *Spekia*: 2.2 GPa).

2.3. FEA model

A structural static analysis was performed employing the finite element package ANSYS 17.1 (Ansys, Canonsburg, USA) in a Dell Precision Workstation T7820 with 64 GB RAM. The radulae were meshed using the ANSYS mesh module with an adaptive mesh of hexahedral elements [96] resulting in about 100,000 elements per model. As result we received qualitative stress and strain distribution plots. Areas of high local stress or strain are coloured in red, of no stress or strain in blue, green and yellow are intermediate (please see scales in the Figs. 5–8). We tested different biomechanical scenarios in function of the value and the direction of the force.

Direction of force:

We applied force always to the cusps of each central and lateral tooth along the anterior-posterior axis of the radula (see Fig. 2). For the marginal teeth, we tested two directions of forces: along the radular anterior-posterior and anterior-medial axes. We detected, as in the previous study on *Spekia* [49] that stress and strain values are smaller, when loaded along the anterior-medial axis. This, together with recent findings obtained from building and moving a physical radular model for *Spekia zonata* [97], suggests that the marginal teeth rather perform an 'inward raking' and are loaded along the radular anterior-medial axis. Therefore, we have chosen this direction of force for both marginal teeth.

Nominal force:

A load of 1 N per tooth was set for the smallest 3D model of *Bridouxia*. To compare the different models, the nominal forces for the other species were determined by calculating $\text{nominal\_force}^{Cleopatra} = (\text{volume}^{Cleopatra}/\text{volume}^{Bridouxia})^{2/3}$ (see Table 1) using *Bridouxia* as a reference. This is the usual procedure to scaling the models to comparable size: keep the differences in the FEA model and apply an appropriate force that generates the effect of removing the influence of the size [98].

Other loading conditions

Additionally we loaded each tooth with 1 N, 0.5 N, and 0.1 N. These force values were chosen since in the previous breaking stress experiments tooth failure was observed between 1 N and 0.5 N, depending on the species [84–85].

Finally, all the models were fixed in the posterior part of the membrane and we included as a fixed displacement the contact areas on the superior marginal, central and lateral and tooth with a hypothetic new row of teeth above.

2.5. Ecology

The information on the preferred feeding substrate was summarized from the literature or from personal comments of collectors in the field (see Table 1). *Lavigeria grandis* and *Spekia zonata* forage on algae attached to rocks (solid substrate), *Cleopatra johnstoni* forages on algae that cover sand or mud (soft substrate), and *Bridouxia grandidieriana* forages on algae from various surfaces: sand, mud, plant surface (mixed substrate).

3. Results

3.1. Morphology of teeth and radular size

The detailed morphology of teeth was previously described in [50]. All marginal teeth (see Figs. 1–4 for tooth images, schematic drawings, and 3D models) are of rather slender shape with elongated styli and possessing a cusp with multiple and rather fine denticles (except for the inner marginal tooth of *Lavigeria grandis*, possessing no denticles). Centrals and laterals of *Cleopatra johnstoni* are of similar shape to the marginal teeth. Central and lateral teeth of *L. grandis* and lateral teeth of *Spekia zonata* possess one broad and prominent central denticle on the cusp, situated on elongated styli. The central tooth of *Spekia* is rather broad with only few small denticles. *Bridouxia grandidieriana* possess a broad central tooth with fine denticles and a rather slender lateral tooth with elongated stylus and cusp exhibiting one prominent denticle and multiple finer ones. The radulae from adult *B. grandidieriana* specimens are the smallest ones (mean width ± standard deviation; 120 ± 7 µm), followed by *C. johnstoni* (220 ± 9 µm), *S. zonata* (250 ± 10 µm), and finally *L. grandis* with the largest radulae (350 ± 11 µm).

3.2. Results of the FEA

3.2.1. Displacement

In *Lavigeria*, *Spekia*, and *Bridouxia* only the marginals, in *Cleopatra* laterals and centrals are displaced during load, whereas all other teeth do not show significant values of displacement (Fig. 4).

3.3.2. Stress and strain in each species and tooth type

The results of the FEA are sorted to species in Figs. 5–8. In *Lavigeria grandis* (Fig. 8), marginal tooth II experiences the highest stress and strain, followed by marginal tooth I, lateral tooth, and finally central tooth. Here the marginal teeth show the highest values of both parameters on their styli, the lateral teeth on their cusps and styli, and the central teeth on their central denticle of the cusp. In *Bridouxia grandidieriana*, the marginal teeth show the highest concentration of stress and strain at the whole length of their styli, both parameters decrease dramatically from the stylus to cusp and basis across a very small area. The lateral teeth experience highest stress and strain at their inner and outer edges of the styli and on their central denticle of the cusp. The central teeth show stress and strain concentrations on their basis and the medial part of the cusp. In *Spekia zonata*, marginals show very high stress/strain concentrations on the styli of the marginal teeth, and only little stress/strain on the lateral tooth cusps and the anterior margin of the central tooth cusps. In *Cleopatra johnstoni* (Fig. 5), we observed a completely different pattern, here the highest stress and strain were obtained for central teeth, followed by the lateral teeth, and finally both marginal teeth. Centrals and laterals show high concentrations of stress and strain on the posterior part of the cusp; the marginals experience stress and strain at the medial and anterior area of the cusps.

3.3.3. Stress and strain for each loading condition

When all models are loaded with the nominal force (forces are corrected for the radular size) the radula of *Bridouxia* possess the largest area with high concentrations of stress and strain, followed by *Cleopatra*, *Spekia*, and finally *Lavigeria* (Figs. 5–8). With decreasing load in each species, stress and strain concentrations are reduced. *Lavigeria* shows very little stress and strain, when loaded with 1 N, *Spekia* and *Cleopatra* little stress and strain, when loaded with 0.5 N, whereas *Bridouxia* still experiences higher stress and strain, even when loaded with 0.1 N.

4. Discussion

4.1. Distribution of stress and strain

When models are loaded with the nominal force (force corrected for radular size) in the FEA, we can directly compare effects on stress and strain distribution between species and between tooth types (Figs. 5–8). When models were loaded with 1 N, 0.5 N, and 0.1 N (forces are not corrected for radular size), similar to the situation in the breakings stress experiments, we can, in contrast, directly see the effect of the radular size on the stress/strain distribution.

Overall, as determined in our previous FEA on the teeth of *Spekia* [49], the simulated stress and strain under nominal force can be explained by the shape of the teeth and the local mechanical properties that were analysed in previous studies [48, 51]. The simulations of the mechanical behaviour are, in most cases, similar to the observed ones, determined by previous breaking stress experiments under wet condition ([84–85]; see Fig. 3 for the areas of failure in the experiment):

Thick, short, and broader teeth, as the centrals and laterals of *Spekia* and *Lavigeria*, are not as prone to deformation and do not show areas of high local stress, which can enable force transmission to the ingesta [see also 25,90]. These teeth are additionally stiffer, leading to a high ability of the material to transmit forces [for the relationship between Young's modulus and force transmission see e.g. 99–102], supporting puncture mechanics and the resistance to failure [see e.g. 103; review on puncture mechanics see 104]. In our breaking stress experiments these teeth could resist higher forces (mean ± standard deviation; *Spekia*, laterals: 799.83 ± 313.47 mN, centrals: 979.50 ± 381.14 mN; *Lavigeria*, laterals: 270.95 ± 87.49 mN, centrals: 700.90 ± 255.52 mN) and were less prone to failure.

The softer, longer, thinner, and slender teeth, in contrast, as the marginals of *Spekia* and *Lavigeria*, the laterals and marginals of *Bridouxia*, and the centrals and laterals of *Cleopatra*, experience higher strain and stress in the FEA. In our previous breaking stress experiments, these teeth could resist less force, showed a high ability of bending, and usually failed (between 83 and 272 mN, depending on the tooth type and species). Overall, models as well as real teeth (a) can deform more easily during interaction with the ingesta, (b) show areas of high stress, and (c) are more prone to failure.

However, even though central teeth of *Bridouxia* are relatively thin, they show lesser concentrations of stress and strain in the simulations and additionally could resist higher forces (329.11 ± 128.06 mN) than marginals (96.08 ± 13.33 mN) in previous breaking stress experiments. This could be explained by their mechanical properties, as they have a higher Young's modulus than the marginals (Fig. 3), and by the morphology of their basis. They are broader thus and possess a large attachment area with the membrane, enabling better stress redistribution [see also 41]. However, the breaking stress experiments also revealed

that the laterals can resist to similar force (315.31 ± 104.99 mN) than the centrals, even though they are narrower and have similar mechanical properties. This inconsistency between the FEA and experiments could be explained by the ability of the wet lateral teeth to bend and rely on the lateral teeth from the adjacent rows, gaining support [for the importance of tooth-tooth interaction see also 87–91]. This collective effect, is however difficult to simulate in the FEA.

Within each heterogeneous tooth, the areas of high local stress and strain also correspond to the values of the Young's modulus. Additionally, the simulated mechanical behaviours of the tooth areas usually reflect real mechanical behaviour observed in breaking stress experiments. Areas that are rather soft, as the styli and bases of the marginals in *Bridouxia*, *Spekia*, and *Lavigeria* and of the laterals in *Bridouxia*, exhibit a high ability to deform both in simulations and experiments. In docoglossan teeth, this bending behaviour of the stylus has also been previously simulated by the FEA [58]. In our simulations, these areas additionally show high local stress, which corresponds to the areas of failure in the experiment (Fig. 3). In contrast, the stiffer cusps did not deform as much as in the experiment and did not show high local stresses in our FEA. For radular teeth, the importance of the heterogeneous distribution of material properties was previously also determined in docoglossan teeth of *Patella* and Polyplacophora; here [8] detected that the tooth's part, interacting in the ingesta, is harder and stiffer, whereas the underlain parts are softer and more flexible [see also 58 for the flexibility of the stylus]. The co-appearance of harder and softer layers probably leads to a reduction of abrasion in the radular cusps [8, 45] as observed in other structures as well [e.g. 54,105]. The flexibility of both the stylus and basis probably serves as a shock absorber, when interacting with obstacles [see also 58,91], a mechanism also previously reported from other biological structures [e.g. 106–180].

For the homogeneous teeth (with similar Young's moduli) of *Cleopatra* we previously detected, that their force-resistance, determined by breaking stress experiments, is the highest in centrals (350.89 ± 49.44 mN), followed by laterals (170.46 ± 32.30 mN), and finally marginals (136.75 ± 16.50 mN). This is contrary to the distributions of stress and strain, obtained from the FEA (here stress and strain are low in the marginals and high in the centrals and laterals). This can be explained by the specific arrangement of teeth: in our models the outer marginal tooth embraces the inner, smaller one, leading to a reduction of high local stress and to a deceased ability of both teeth to deform together. This is the configuration that can be often observed in the SEM (Fig. 1E). In our previous breaking stress experiments, radulae were extracted from the specimens, taped onto glass objects slides, and teeth were stroked into the proposed feeding position. During this latest step, marginal teeth were unfortunately separated in many cases, thus breaking stress experiments were performed with individual and not with naturally interlocking teeth. If and to which extend embracing teeth can resist to higher force should be studied in further experiments. Within *Cleopatra*'s teeth, we detected high stress and strain at the area between each cusp and stylus, which is in contrast to the experiments, where failure occurred between the stylus and basis (Fig. 3). This can be also explained by the position of teeth in the simulations, as each stylus has a relatively large area of contact with the adjacent stylus from the same tooth type, leading to a distribution of stress across the styli to the underlain radular membrane, but also reducing the stylus' ability to deform.

When stresses are not corrected for size, we detect, as expected, that smaller radulae show more stress and strain than larger ones, with *Bridouxia* showing the highest local concentrations of stress/strain, followed by *Cleopatra*, *Spekia*, and finally *Lavigeria* with the lowest ones. Even though the FEA does not allow direct conclusions about failure behaviour or force-resistance of structures, we can suggest the presence of some relationship between the breaking forces, determined in the experiments, with the stress simulations under the defined loads (1 N, 0.5 N, 0.1 N). In the experiment, *Cleopatra*'s teeth were able to resist to maximal 400 mN (comparable to FEA, loaded with 0.5 N), *Bridouxia*'s to 460 mN (comparable to FEA, loaded with 0.5 N), *Lavigeria*'s to 956 mN (comparable to FEA, loaded with 1 N), and *Spekia*'s to 1360 mN (comparable to FEA, loaded with 1 N). When the stress scales of the FEA models are considered, structural failure should actually occur, when areas of the modelled teeth experience between 1 to 6 MPa. However, as mentioned above, *Spekia* is able to resist to the highest forces in real experiments, followed by *Lavigeria*, *Bridouxia*, and finally *Cleopatra*. This already indicates that besides the parameter size, other factors seem to be important to reduce stress and strain in living radula. Our here presented models have distinct local Young's moduli, but are modelled as filled solid bulk materials. Real teeth are, however, composed of fibres and their arrangement, size, and density seem to contribute to the reinforcement of the tooth itself, as it was detected for limpet and chiton teeth [44–46, 109–114]. These parameters, however, await further investigations in the paludomid teeth.

4.2. Functional and trophic specialisations of tooth types

Padilla [90] summarized previous approaches on radular function and proposed new avenues to gain deeper insight into its functionality and in general to molluscan ecology. She highlighted the importance of the 3D shape, material properties, and interaction of teeth.

By the here presented results of the FEA, that include these parameters, we were able to verify previous hypotheses about tooth functionalities in paludomid gastropods. In soft substrate feeders, all teeth are rather used for collecting particles (monofunctional radula; [51, 85]), whereas in mixed and solid substrate feeders, the centrals and laterals rather loosen food from the substrate, and the marginals collect the particles afterwards (multifunctional radula; [48, 51, 85]. This is supported, as mentioned above, by the simulated mechanical behaviour of teeth under nominal force [see also 49 for *Spekia*]: the centrals and laterals of *Lavigeria* and *Spekia* are rather capable of transferring forces without deformation. The marginals show, in contrast, a high capability of bending at the basis and the stylus, which results in the reduction of failure, but also does not facilitate a direct transfer of forces from the radula to the food. They probably gather the loosened particles in form of an 'inward raking' during retraction of the radula from the ingesta [see 27]. This hypothesis is also supported by another previous approach, involving a physical radular model of *Spekia* [97]. In that study, we performed dissections of adult specimens, extracted the whole buccal mass with the musculature and radula, documented the anatomy, and mimicked the structures by 3D printing and assembly of fabrics. With this approach, we were able to build the first, relatively simple, but movable radular model. By the manipulation of the radular supporting structures of the model the interaction and ranges of motion of the radular structures could be documented. Hereby we found that the marginal teeth are flexed as consequence from a rotation of the underlain buccal mass musculature and perform a raking motion from the middle of the radula to the outer edges, an 'inward raking'.

A high ability of bending and the presence of areas of high local stress, leading to a higher risk of breaking, was also simulated by the FEA on the centrals and laterals of *Cleopatra*. For taenioglossan radulae, it was previously hypothesized that the central teeth are rather used for gathering food [27, 115–116], which seems to be the case for *Cleopatra*, but, as mentioned above, not for *Lavigeria* and *Spekia*. Thus, the functionality of certain tooth types varies greatly between species. We however, also detected by the FEA that the marginals of *Cleopatra*, when arranged in an embracing position, show less stress and strain. This

indicates that in this species marginals are potentially more effective in forcefully loosening algae, which was previously also proposed for the marginal teeth of *Littorina* [117].

As mentioned above, we determined by the FEA that with increasing radular size, stress and strain decreases. However, in previous experiments, teeth of *Spekia* could resist higher forces than those of *Lavigeria*, and *Bridouxia* - higher forces than *Cleopatra* [85]. We therefore propose that the observed size differences between the species studied are the result of adaptations to distinct algae cover types rather than an assistance in foraging on the same algae cover, but with a greater food loosening ability due to larger contact areas between tooth and ingesta. To test this hypothesis, however, the identification, sampling, and finally mechanical testing of the biofilm and algal coverage in Lake Tanganyika is necessary.

Declarations

Authors' contribution

WK and SG initiated and designed the study and discussed the data. WK created the 3Ds of *Cleopatra* and *Lavigeria*, remodelled *Bridouxia* and *Spekia*, and wrote the manuscript draft, which was discussed and revised by JMN and SG. JMN prepared the models for ANSYS, plotted the Young's moduli, and conducted the finite-elements-analysis. All authors contributed to and approved the final version of the manuscript for publication.

Acknowledgements

We would like to acknowledge Nicole Wolff and Hasan Karabacak from the CeNak, University of Hamburg, for providing the 3D models of *Bridouxia grandidieriana* and *Spekia zonata*. We would like to thank Heinz Büscher from Basel for collecting specimens at Lake Tanganyika, Matthias Glaubrecht from the CeNak, University of Hamburg, for the comments on molluscan biology in previous studies, and Thomas M. Kaiser from the CeNak, University of Hamburg, for discussion on some results. JMN acknowledges the Serra-Hunter and the CERCA programme of the Generalitat de Catalunya. We are grateful for the comments of the four anonymous reviewers and the editorial office.

Funding

This research did not receive any specific grant from funding agencies in the public, commercial, or not-for-profit sectors.

References

1. Ankel, W. E. Erwerb und Aufnahme der Nahrung bei den Gastropoden. *Verh. Dtsch. Zool. Ges., Zool. Anz*, **11**, 223–295 (1938).
2. Eigenbrodt, H. Untersuchungen über die Funktion der Radula einiger Schnecken. *Z. Morphol. Oekol. Tiere*, **37**, 735–791 (1941).
3. Crampton, D. Functional anatomy of the buccal apparatus of Onchidoris bilamellata (Mollusca: Opisthobranchia. *Trans. Zool. Soc. Lond*, **34**, 45–86 https://doi.org/10.1111/j.10963642.1977.tb00372.x (1977).
4. Wägele, H. Rasterelektronenmikroskopische Untersuchungen an Radulae einiger Nordseeschnecken (Gastropoda: Prosobranchia) mit Anmerkungen zur Funktionsmorphologie. *Drosera*, **83**, 68–78 (1983).
5. Hawkins, S. J. *et al.* A. A comparison of feeding mechanisms in microphagus, herbivorous, intertidal, Prosobranchs in relation to resource partitioning. *J. Molluscan Stud*, **55**, 151–165 (1989).
6. Scheel, C., Gorb, S. N., Glaubrecht, M. & Krings, W. Not just scratching the surface: distinct radular motion patterns in Mollusca. Biol. Open 9, bio.055699(2020). https://doi.org/10.1242/bio.055699
7. Runham, N. W. & Thornton, P. R. Mechanical wear of the gastropod radula: a scanning electron microscope study. *J. Zool*, **153**, 445–452 https://doi.org/10.1111/j.1469-7998.1967.tb04976.x (1967).
8. van der Wal, P., Giesen, H. & Videler, J. Radular teeth as models for the improvement of industrial cutting devices. *Mater. Sci. Eng. C*, **7**, 129–142 (2000).
9. Shaw, J. A., Macey, D. J., Brooker, L. R. & Clode, P. L. Tooth use and wear in three iron-biomineralizing mollusc species. *Biol. Bull*, **218**, 132–144 (2010).
10. Ukmar-Godec, T., Kapun, G., Zaslansky, P. & Faivre, D. The giant keyhole limpet radular teeth: A naturally-grown harvest machine. *J. Struct. Biol*, **192**, 392–402 https://doi.org/10.1016/j.jsb.2015.09.021 (2015).
11. Mikovari, A. *et al.* Radula development in the giant key-hole limpet Megathura crenulata. *J. Shellfish Res*, **34**, 893–902 https://doi.org/10.2983/035.034.0319 (2015).
12. Krings, W. & Gorb, S. N. Substrate roughness induced wear pattern in gastropod radulae. *Biotribology*, **26**, 100164 https://doi.org/10.1016/j.biotri.2021.100164 (2021).
13. Krings, W. *et al.* experiments on Vittina turrita (Mollusca, Gastropoda, Neritidae) reveal tooth contact areas and bent radular shape during foraging. Sci. Rep. 11, 9556(2021). https://doi.org/10.1038/s41598-021-88953-7
14. Runham, N. W. Rate of replacement of the molluscan radula. *Nature*, **194**, 992–993 https://doi.org/10.1038/194992b0 (1962).
15. Runham, N. W. & Isarankura, K. Studies on radula replacement. *Malacologia*, **5**, 73 (1966).
16. Mackenstedt, U. & Märkel, K. Experimental and comparative morphology of radula renewal in pulmonates (Mollusca, Gastropoda)., **107**, 209–239 https://doi.org/10.1007/BF00312262 (1987).
17. Padilla, D. K., Dittman, D. E., Franz, J. & Sladek, R. Radular production rates in two species of Lacuna Turton (Gastropoda: Littorinidae). *J. Molluscan Stud*, **62**, 275–280 https://doi.org/10.1093/mollus/62.3.275 (1996).

18. Shaw, J. A., Macey, D. J. & Brooker, L. R. Radula synthesis by three species of iron mineralizing molluscs: production rate and elemental demand. *J. Mar. Biol. Assoc. U.K*, **88**, 597–601 https://doi.org/10.1017/S0025315408000969 (2008).
19. Vortsepneva, E., Herbert, D. G. & Kantor, Y. Radula formation in two species of Conoidea (Gastropoda).*J. Morphol.*281,1328–1350*(*2020*).* https://doi.org/10.1002/jmor.21250
20. Solem, A. Patterns of radular tooth structure in carnivorous land snails. *Veliger*, **17**, 81–88 (1974).
21. Walsby, J. R. Feeding and the radula in the marine pulmonate limpet, Trimusculus reticulatus. *Veliger*, **18**, 139–145 (1975).
22. Jensen, K. R. A review of sacoglossan diets, with comparative notes on radular and buccal anatomy. *Malacological Review*, **13**, 55–77 (1980).
23. Jensen, K. R. Observations on feeding methods in some Florida ascoglossans. *J. Molluscan Stud*, **47**, 190–199 (1981).
24. Jensen, K. R. Factor affecting feeding selectivity in herbivorous Ascoglossa (Mollusca: Opisthobranchia). *J. Exp. Mar. Biol. Ecol*, **66**, 135–148 https://doi.org/10.1016/00220981(83)90035-7 (1983).
25. Jensen, K. R. Morphological adaptations and plasticity of radular teeth of the Sacoglossa (= Ascoglossa) (Mollusca: Opisthobranchia) in relation to their food plants. *Biol. J. Linn. Soc*, **48**, 135–155 https://doi.org/10.1111/j.1095-8312.1993.tb00883.x (1993).
26. Jensen, K. R. Evolution of the Sacoglossa (Mollusca, Opisthobranchia) and the ecological associations with their food plants. *Evol. Ecol*, **11**, 301–335 https://doi.org/10.1023/A:1018468420368 (1997).
27. Steneck, R. S. & Watling, L. Feeding capabilities and limitation of herbivorous molluscs: a functional group approach. *Mar. Biol*, **68**, 299–319 https://doi.org/10.1007/BF00409596 (1982).
28. Burch, J. B. & Jeong, K. H. The radula teeth of selected Planorbidae. *Malacological Review*, **17**, 67–84 (1984).
29. Kesler, D. H., Jokinen, E. H. & Munns, W. R. Jr. Trophic preferences and feeding morphology of two pulmonate snail species from a small New England pond, USA. *Can. J. Zool*, **64**, 2570–2575 https://doi.org/10.1139/z86-377 (1986).
30. Black, R., Lymbery, A. & Hill, A. Form and function: size of radular teeth and inorganic content of faeces in a guild of grazing molluscs at Rottnest Island, Western Australia. *J. Exp. Mar. Biol. Ecol*, **121**, 23–35 https://doi.org/10.1016/0022-0981(88)90021-4 (1988).
31. Bleakney, J. S. Indirect evidence of a morphological response in the radula of Placida dentritica (Alder and Hancock, 1843) (Opisthobranchia, Ascoglossa/ Sacoglossa) to different algae prey. *Veliger*, **33**, 111–115 (1990).
32. Padilla, D. K. Inducible phenotypic plasticity of the radula in Lacuna (Gastropoda: Littorinidae). *Veliger*, **41**, 201–204 (1998).
33. Reid, D. G. & Mak, Y. M. Indirect evidence for ecophenotypic plasticity in radular dentition of Littoraria species (Gastropoda: Littorinidae). *J. Molluscan Stud*, **65**, 355–370 https://doi.org/10.1093/mollus/65.3.355 (1999).
34. Nishi, M. & Kohn, A. J. Radular teeth of Indo-Pacific molluscivorous species of Conus: a comparative analysis. *J. Molluscan Stud*, **65**, 483–497 https://doi.org/10.1093/mollus/65.4.483 (1999).
35. Padilla, D. K., Dilger, E. K. & Dittmann, D. E. Phenotypic plasticity of feeding structures in species of Littorina. *Am. Zool*, **40**, 1161–1161 (2000).
36. Duda, T. F., Kohn, A. J. & Palumbi, S. R. Origins of diverse feeding ecologies within Conus, a genus of venomous marine gastropods. *Biol. J. Linn. Soc*, **73**, 391–409 https://doi.org/10.1006/bijl.2001.054 (2001).
37. Ito, A., Ilano, A. S. & Nakao, S. Seasonal and tidal height variations in body weight and radular length in *Nodilittorina radiata* (Eydoux & Souleyet, 1852). *J. Molluscan Stud.* **68**, 197–203 (2002). https://doi.org/10.1093/mollus/68.3.197
38. von Rintelen, T., Wilson, A. B., Meyer, A. & Glaubrecht, M. Escalation and trophic specialization drive adaptive radiation of freshwater gastropods in ancient lakes on Sulawesi, Indonesia. Proc. R. Soc. Lond. 271, 2541–2549(2004). https://doi.org/10.1098/rspb.2004.2842
39. Ramesh, R. & Ravichandran, S. Feeding biology with reference to algal preference and scanning electron microscopy studies on the radula of Turbo brunneus. *Trends Appl. Sci. Res*, **3**, 189–195 https://doi.org/10.3923/tasr.2008.189.195 (2008).
40. Krings, W. Trophic specialization of paludomid gastropods from 'ancient' Lake Tanganyika reflected by radular tooth morphologies and material properties. Dissertation, 2020. https://ediss.sub.uni-hamburg.de/handle/ediss/8654
41. Krings, W., Brütt, J. O., Gorb, S. N. & Glaubrecht, M. Tightening it up: Diversity of the chitin anchorage of radular teeth in paludomid freshwater gastropods. *Malacologia*, **63**, 77–94 https://doi.org/10.4002/040.063.0108 (2020).
42. Breure, A. S. H. & Gittenberger, E. The rock-scraping radula, a striking case of convergence (Mollusca). *Neth. J. Zool*, **32**, 307–312 https://doi.org/10.1163/002829681X00347 (1981).
43. Weaver, J. C. *et al.* Analysis of an ultra hard magnetic biomineral in chiton radular teeth. *Mater. Today*, **13**, 42–52 https://doi.org/10.1016/S1369-7021(10)70016-X (2010).
44. Lu, D. & Barber, A. H. Optimized nanoscale composite behaviour in limpet teeth. *J. Royal Soc. Interface*, **9**, 1318–1324 https://doi.org/10.1098/rsif.2011.0688 (2012).
45. Grunenfelder, L. K. *et al.* Stress and damage mitigation from oriented nanostructures within the radular teeth of Cryptochiton stelleri. *Adv. Funct. Mater*, **24/39**,, 6085 https://doi.org/10.1002/adfm.201401091 (2014).
46. Barber, A. H., Lu, D. & Pugno, N. M. Extreme strength observed in limpet teeth. *J. Royal Soc. Interface*, **12**, 20141326 https://doi.org/10.1098/rsif.2014.1326 (2015).
47. Ukmar-Godec, T. *et al.* Materials nanoarchitecturing via cation-mediated protein assembly: Making limpet teeth without mineral. *Adv. Mater*, **29**, 1701171 https://doi.org/10.1002/adma.201701171 (2017).
48. Krings, W., Kovalev, A., Glaubrecht, M. & Gorb, S. N. Differences in the Young modulus and hardness reflect different functions of teeth within the taenioglossan radula of gastropods. *Zoology*, **137**, 125713 https://doi.org/10.1016/j.zool.2019.125713 (2019).

49. Krings, W., Marcé-Nogué, J., Karabacak, H., Glaubrecht, M. & Gorb, S. N. Finite element analysis of individual taenioglossan radula teeth. *Acta Biomater*, **115**, 317–332 https://doi.org/10.1016/j.actbio.2020.08.034 (2020).
50. Krings, W., Neiber, M. T., Kovalev, A., Gorb, S. N. & Glaubrecht, M. Trophic specialisation reflected by radular tooth material properties in an 'ancient' Lake Tanganyikan gastropod species flock. *BMC Ecol. Evo*, **21**, 35 https://doi.org/10.1186/s12862-021-01754-4 (2021).
51. Gorb, S. N. & Krings, W. Mechanical property gradients of taenioglossan radular teeth are associated with specific function and ecological niche in Paludomidae (Gastropoda: Mollusca). *Acta Biomater*, https://doi.org/ 10.1016/j.actbio.2021.07.057 (2021).
52. Aifantis, E. C. On the role of gradients in the localization of deformation and fracture.*Int. J. Eng. Sci.*3,1279–1299*(*1992*).* https://doi.org/10.1016/ 0020-7225(92)90141-3
53. Bingbing, A., Wang, R., Arola, D. & Zhang, D. The role of property gradients on the mechanical behavior of human enamel.*J. Mech. Behav. Biomed. Mater.*9,63–72*(*2012*).* https://doi.org/10.1016/j.jmbbm.2012.01.009
54. Michels, J., Vogt, J. & Gorb, S. N. Tools for crushing diatoms — opal teeth in copepods feature a rubber-like bearing composed of resilin.*Sci. Rep.*2,465*(* 2012*).*
55. Liu, Z. *et al.* Enhanced protective role in materials with gradient structural orientations: lessons from nature.*Acta Biomater.*44,31–40*(*2016*).* https://doi.org/10.1016/j.actbio.2016.08.005
56. Büsse, S. & Gorb, S. N. Material composition of the mouthpart cuticle in a damselfly larva (Insecta: Odonata) and its biomechanical significance.*R. Soc. Open Sci.*5,172117*(*2018*).*
57. Saltin, B. D. *et al.* Material stiffness variation in mosquito antennae.*J. R. Soc. Interface*16,20190049*(*2019*).* https://doi.org/10.1098/rsif.2019.0049
58. Pohl, A. *et al.* Radular stylus of Cryptochiton stelleri: A multifunctional lightweight and flexible fiber-reinforced composite. *J. Mech. Behav. Biomed. Mater*, **111**, 103991 (2020).
59. Boss, K. J. On the evolution of gastropods in ancient lakes in Pulmonates Systematics, Evolution and Ecology, vol. 2a (eds. Fretter, V., Peake, J.) 385–428(Academic Press, London, 1978).
60. Johnston, M. R. & Cohen, A. S. Morphological divergence in endemic gastropods from Lake Tanganyika: implications for models of species flock formation., **2**, 413–425 https://doi.org/10.2307/3514613 (1987).
61. Coulter, G. W. *Lake Tanganyika and its life* (Oxford University Press, Oxford, 1991).
62. Michel, E., Cohen, A. S., West, K., Johnston, M. R. & Kat, P. W. Large African lakes as natural laboratories for evolution: examples from the endemic gastropod fauna of Lake Tanganyika. *Mitt. Internat. Verein. Limnol*, **23**, 85–99 https://doi.org/10.1080/05384680.1992.11904012 (1992).
63. Michel, E.. Why snails radiate: a review of gastropod evolution in long-lived lakes, both recent and fossil in Speciation in ancient lakes, Advances in Limnology (eds. Martens, K., Goddeeris, B., Coulter, G. W.)285–317(E. Schweizerbart'sche Verlagsbuchhandlung, Stuttgart, 1994).
64. Michel, E. Phylogeny of a gastropod species flock: exploring speciation in Lake Tanganyika in a molecular framework. *Adv. Ecol. Res*, **31**, 275–302 https://doi.org/10.1016/S0065-2504(00)31016-9 (2000).
65. Martens, K. Speciation in ancient lakes. *Trends. Ecol. Evol*, **12**, 177–182 https://doi.org/10.1016/S0169-5347(97)01039-2 (1997).
66. West, K. & Michel, E. The dynamics of endemic diversification; molecular phylogeny suggests an explosive origin of the thiarid gastropods of Lake Tanganyika. *Adv. Ecol. Res*, **31**, 331–354 https://doi.org/10.1016/S0065-2504(00)31018-2 (2000).
67. Wilson, A. B., Glaubrecht, M. & Meyer, A. Ancient lakes as evolutionary reservoirs: evidence from the thalassoid gastropods of Lake Tanganyika. Proc. Royal Soc. Lond. B 271, 529–536(2004). https://doi.org/10.1098/rspb.2003.2624
68. Glaubrecht, M. Adaptive radiation of thalassoid gastropods in Lake Tanganyika, East Africa: morphology and systematization of a paludomid species flock in an ancient lake. *Zoosystematics Evol*, **84**, 71–122 https://doi.org/10.1002/zoos.200700016 (2008).
69. West, K., Michel, E., Todd, J., Brown, D. & Clabaugh, J. *The Gastropods of Lake Tanganyika: Diagnostic key, classification and notes on the fauna* (Societas Internationalis Limnologiae - Int. Assoc. of Theoretical and Applied Limnology, Special publications, 2003).
70. Fortuny, J., Marcé-Nogué, J., de Esteban-Trivigno, S., Gil, L. & Galobart, Ã. Temnospondyli bite club: ecomorphological patterns of the most diverse group of early tetrapods. *J. Evol. Biol*, **24**, 2040–2054 https://doi.org/10.1111/j.1420-9101.2011.02338.x (2011).
71. Fortuny, J., Marcé-Nogué, J. & Konietzko-Meier, D. Feeding biomechanics of Late Triassic metoposaurids (Amphibia: Temnospondyli): a 3D finite element analysis approach. *J. Anat*, **230**, 752–765 https://doi.org/10.1111/joa.12605 (2017).
72. Neenan, J. M., Ruta, M., Clack, J. A. & Rayfield, E. J. Feeding biomechanics in Acanthostega and across the fish-tetrapod transition. Proc. R. Soc. B 281, 20132689(2014). http://doi.org/10.1098/rspb.2013.2689
73. Figueirido, B., Tseng, Z. J., Serrano-Alarcon, F. J., Martin-Serra, A. & Pastor, J. F. F. Three-dimensional computer simulations of feeding behaviour in red and giant pandas relate skull biomechanics with dietary niche partitioning. *Biol. Lett*, **10**, 20140196 https://doi.org/10.1098/rsbl.2014.0196 (2014).
74. Soons, J. *et al.* Is beak morphology in Darwin's Finches tuned to loading demands? *PLOS ONE*, **10**, e0129479 https://doi.org/10.1371/journal.pone.0129479 (2015).
75. Maiorino, L., Farke, A. A., Kotsakis, T., Teresi, L. & Piras, P. Variation in the shape and mechanical performance of the lower jaws in ceratopsid dinosaurs (Ornithischia, Ceratopsia). *J. Anat*, **227**, 631–646 https://doi.org/10.1111/joa.12374 (2015).
76. Serrano-Fochs, S., de Esteban-Trivigno, S., Marcé-Nogué, J., Fortuny, J. & Fariña, R. A. Finite element analysis of the Cingulata jaw: an ecomorphological approach to Armadillo's diets. *PLOS ONE*, **10**, e0120653 https://doi.org/10.1371/journal.pone.0129953 (2015).
77. Marcé-Nogué, J., Fortuny, J., Gil, L. & Sánchez, M. Improving mesh generation in finite element analysis for functional morphology approaches. *Span. J. Palaeontol*, **31**, 117–132 (2015).

78. Marcé-Nogué, J., Püschel, T. A. & Kaiser, T. M. A biomechanical approach to understand the ecomorphological relationship between primate mandibles and diet. *Sci. Rep*, **7**, 8364 https://doi.org/10.1038/s41598-017-08161-0 (2017).
79. Konietzko-Meier, D., Gruntmejer, K., Marcé-Nogué, J., Bodzioch, A. & Fortuny, J. Merging cranial histology and 3D-computational biomechanics: a review of the feeding ecology of a Late Triassic temnospondyl amphibian. *PeerJ*, **6**, e4426 https://doi.org/10.7717/peerj.4426 (2018).
80. Zhou, Z., Winkler, D. E., Fortuny, J., Kaiser, T. M. & Marcé-Nogué, J. Why ruminating ungulates chew sloppily: Biomechanics discern a phylogenetic pattern. *PLOS ONE*, **14**, e0214510 https://doi.org/10.1371/journal.pone.0214510 (2019).
81. Klunk, C. L., Argenta, M. A., Casadei-Ferreira, A., Economo, E. P. & Pie, M. R. Mandibular morphology, task specialization and bite mechanics in Pheidole ants (Hymenoptera: Formicidae).*J. R. Soc. Interface*18,20210318*(*2021*).* http://doi.org/10.1098/rsif.2021.0318
82. Ballell, A. & Ferrón, H. G. Biomechanical insights into the dentition of megatooth sharks (Lamniformes: Otodontidae). *Sci. Rep*, **11**, 1232 https://doi.org/10.1038/s41598-020-80323-z (2021).
83. Miura, S., Saito, R., Parque, V. & Miyashita, T. Design factors for determining the radula shape of Euhadra Peliomphala. Sci. Rep. 9, 749(2019). https://doi.org/10.1038/s41598-018-36397-x
84. Krings, W., Kovalev, A. & Gorb, S. N. Influence of water content on mechanical behaviour of gastropod taenioglossan radulae. Proc. R. Soc. B 288, 20203173(2021). https://doi.org/10.1098/rspb.2020.3173
85. Krings, W., Kovalev, A. & Gorb, S. N. Collective effect of damage prevention in taenioglossan radular teeth is related to the ecological niche in Paludomidae (Gastropoda: Cerithioidea). *Acta Biomater*, https://doi.org/10.1016/j.actbio.2021.07.073 (2021).
86. Solem, A. Malacological applications of scanning electron microscopy II. Radular structure and functioning. *Veliger*, **14**, 327–336 (1972).
87. Hickman, C. S. Gastropod radulae and the assessment of form in evolutionary paleontology. *Paleobiology*, **6**, 276–294 (1980).
88. Hickman, C. S. Implications of radular tooth-row functional integration for archaeogastropod systematics. *Malacologia*, **25**, 143–160 (1984).
89. Morris, T. E. & Hickman, C. S. A method for artificially protruding gastropod radulae and a new model of radula function. *Veliger*, **24**, 85–89 (1981).
90. Padilla, D. K. Form and function of radular teeth of herbivorous molluscs: Focus on the future. *Am. Malacolog. Bull*, **18**, 163–168 (2003).
91. Herrera, S. A. *et al.* Stylus support structure and function of radular teeth in *Cryptochiton stelleri*. 20th International Conference on Composite Materials Copenhagen, 19–24th July 2015.
92. Holznagel, W. A nondestructive method for cleaning gastropod radulae from frozen, alcohol-fixed, or dried material. *Am. Malacol. Bull*, **14** (2), 181–183 (1998).
93. Oliver, W. C. & Pharr, G. M. An improved technique for determining hardness and elastic modulus using load and displacement sensing indentation experiments. *J. Mater. Res*, **7**, 1564–1583 https://doi.org/10.1557/JMR.1992.1564 (1992). https://doi
94. Davis, J. L., Dumont, E. R., Strait, D. S. & Grosse, I. R. An efficient method of modeling material properties using a thermal diffusion analogy: An example based on craniofacial bone. *PLOS ONE*, **6**, e17004 https://doi.org/10.1371/journal.pone.0017004 (2011).
95. Smith, A. L. *et al.* The feeding biomechanics and dietary ecology of Paranthropus boisei. *Anat. Rec*, **298**, 145–167 https://doi.org/10.1002/ar.23073 (2014).
96. Marcé-Nogué, J. *et al.* À. 3D computational mechanics elucidate the evolutionary implications of orbit position and size diversity of early amphibians. PLOS ONE 10, e0131320(2015). https://doi.org/10.1371/journal.pone.0131320
97. Krings, W., Karabacak, H. & Gorb, S. N. From the knitting shop: the first physical model of the taenioglossan radula (Mollusca: Gastropoda) aids in unravelling functional principles of the radular morphology. In press at Journal of the Royal Society Interface.
98. Marcé-Nogué, J.. Mandibular biomechanics as a key factor to understand diet in mammals in Mammalian teeth – form and function (eds. Martin, T., Koenigswald, W. V.),54–80(Verlag Dr. Friedrich Pfeil, München, 2020). https://doi.org/10.23788/mammteeth.04
99. Bendsøe, M. P. Optimal shape design as a material distribution problem. *Struct. Optim*, **1**, 193–202 (1989).
100. Bendsøe, M. P. *Optimization of Structural Topology, Shape and Material* (Springer, Berlin, 1995).
101. Bendsøe, M. P. & Kikuchi, N. Generating optimal topologies in structural design using a homogenization method. *Comput. Methods Appl. Mech. Eng*, **71**, 197–224 (1988).
102. Dumont, E. R., Grosse, I. R. & Slater, G. J. Requirements for comparing the performance of finite element models of biological structures. *J. Theor. Biol*, **256**, 96–103 (2009).
103. Freeman, P. W. & Lemen, C. A. The trade-off between tooth strength and tooth penetration: predicting optimal shape of canine teeth. *J. Zool*, **273**, 273–280 (2007).
104. Anderson, P. S. L. Making a point: shared mechanics underlying the diversity of biological puncture. *J. Exp. Biol*, **221**, jeb187294 https://doi.org/10.1242/jeb.187294 (2018).
105. Klein, M., -, C. G. & Gorb, S. N. Epidermis architecture and material properties of the skin of four snake species. *J. R. Soc. Interface*, **9**, 3140–3155 https://doi.org/10.1098/rsif.2012.0479 (2012).
106. Haas, F., Gorb, S. N. & Blickhan, R. The function of resilin in beetle wings. Proc. R. Soc. B 267, 1375–1381(2000). https://doi.org/10.1098/rspb.2000.1153
107. Miserez, A., Schneberk, T., Sun, C., Zok, F. W. & Waite, J. H. The transition from stiff to compliant materials in squid beaks., **319**, 1816–1819 (2008).
108. Rajabi, H., Shafiei, A., Darvizeh, A. & Gorb, S. N. Resilin microjoints: a smart design strategy to avoid failure in dragonfly wings. *Sci. Rep*, **6**, 39039 https://doi.org/10.1038/srep39039 (2016).
109. Evans, L. A., Macey, D. J. & Webb, J. Characterization and structural organization of the organic matrix of radula teeth of the chiton Acanthopleura hirtosa. *Philos. Trans. R. Soc. Lond. B*, **329**, 87–96 (1990).

110. Evans, L. A., Macey, D. J. & Webb, J. Matrix heterogeneity in the radular teeth of the chiton Acanthopleura hirtosa. *Acta Zool*, **75**, 75–79 (1994).
111. Wealthall, R. J., Brooker, L. R., Macey, D. J. & Griffin, B. J. Fine structure of the mineralized teeth of the chiton Acanthopleura echinata (Mollusca: Polyplacophora). *J. Morphol*, **265**, 165–175 (2005).
112. Gordon, L. & Joester, D. Nanoscale chemical tomography of buried organic–inorganic interfaces in the chiton tooth. *Nature*, **469**, 194–198 (2011).
113. Huang, W. *et al.* Multiscale Toughening Mechanisms in Biological Materials and Bioinspired Designs. *Adv. Mater*, **31**, 1901561 https://doi.org/10.1002/adma.201901561 (2019).
114. Stegbauer, L. *et al.* Persistent polyamorphism in the chiton tooth: From a new biomineral to inks for additive manufacturing. *PNAS*, **118**, e2020160118 (2021).
115. Fretter, V. & Graham, A. *British prosobranch mollusca, their functional anatomy and ecology* (Ray Society, London, 1962).
116. Jüch, P. J. W. & Boeksehoten, G. J. Trace fossils and grazing traces produced by Littorina and Lepidochitona. *Dutch Wadden Sea, Geologie en Mijnbouw*, **59**, 33–42 (1980).
117. Reid, D. G. *Systematics and evolution of Littorina* (Ray Society, London, 1996).
118. Germain, L. Mollusques du Lac Tanganyika et de ses environs. Extrait des resultats secientifiques des voyages en Afrique d'Edouard Foa. *Bull. Mus. Natl. Hist. Nat*, **14**, 1–612 (1908).
119. Bandel, K. Evolutionary history of East African fresh water gastropods interpreted from the fauna of Lake Tanganyika and Lake Malawi. *Zbl. Geol. Paläont. Teil*, **I**, 233–292 (1997).
120. Bourguignat, M. J. R. *Notice prodromique sur les mollusques terrestres et fluviatiles* (Savy, Paris, 1885).
121. Bourguignat, M. J. R. *Iconographie malacologiques des animaux mollusques fluviatiles du Lac Tanganika* (Corbeil, Créte, 1888).
122. Pilsbry, H. A. & Bequaert, J. The aquatic mollusks of the Begian Congo. With a geographical and ecological account of Congo malacology. *Bull. Am. Mus. Nat. Hist*, **53**, 69–602 (1927).
123. Leloup, E. Exploration Hydrobiologique du Lac Tanganika (1946–1947)(Bruxelles, 1953).
124. Brown, D. *Freshwater snails of Africa and their medical importance* (Taylor and Francis, London, 1994).

Figures

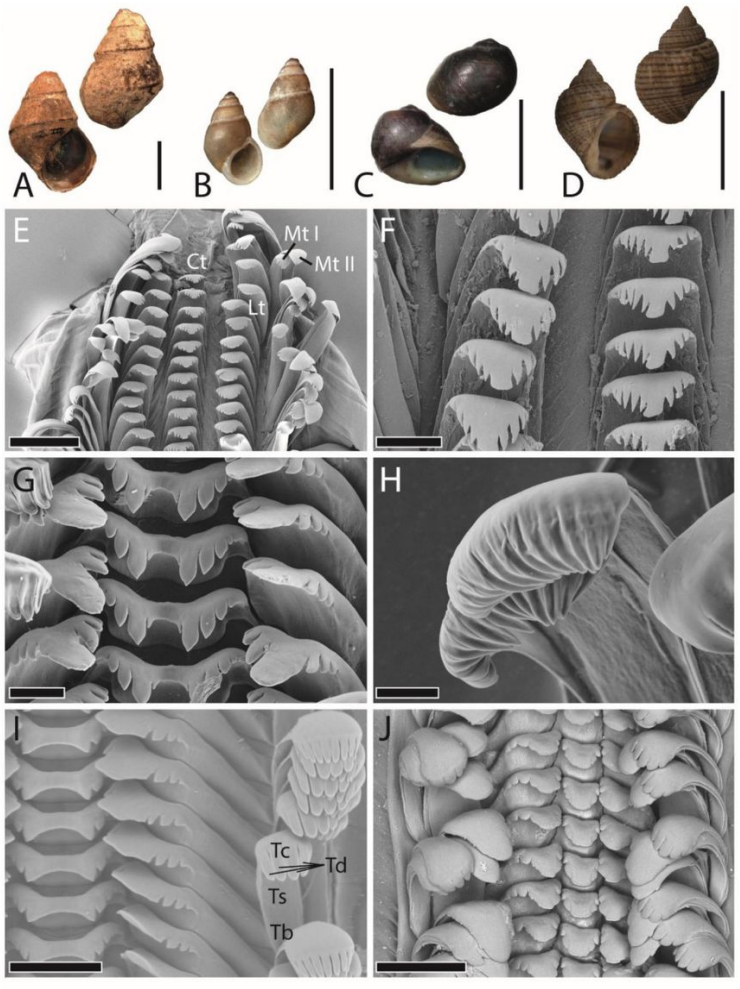

Figure 1

A–D. Shells of adult specimens (adapted from [50,84]). A. Cleopatra johnstoni, B. Bridouxia grandidieriana, C. Spekia zonata, D. Lavigeria grandis. E–J. SEM images of the working zone from adult specimens (G. and J. adapted from [50,84]). Ct = central tooth, Lt = lateral tooth, Mt I = marginal tooth I (inner marginal tooth), Mt II = marginal tooth II (outer marginal tooth), TB = tooth basis, Tc = tooth cusp, Td = tooth denticles, Ts = tooth stylus. Scale bars: A–B = 5 mm, C = 10 mm, F = 20 mm, E, J = 200 μm, F = 60 μm, G = 20 μm, H = 8 μm, I = 100 μm.

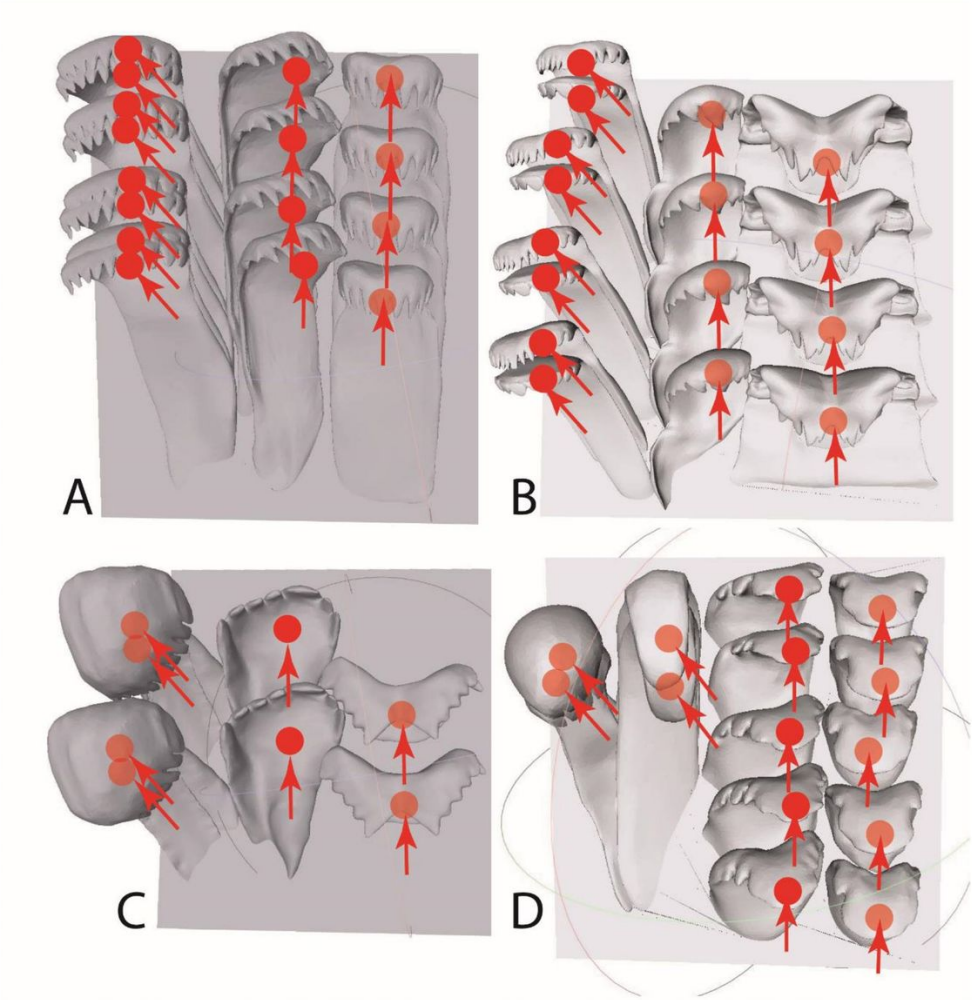

Figure 2

3D models, before creating symmetry, generated in accordance with SEM images from top view (visualized with Meshlab 2016). A. Cleopatra johnstoni, B. Bridouxia grandidieriana, C. Spekia zonata, D. Lavigeria grandis. Red dots highlight the areas that were loaded by FEA, always at the inner area of the cusps. Arrows indicate the direction of force applied (along the anterior-posterior or anterior-medial axis).

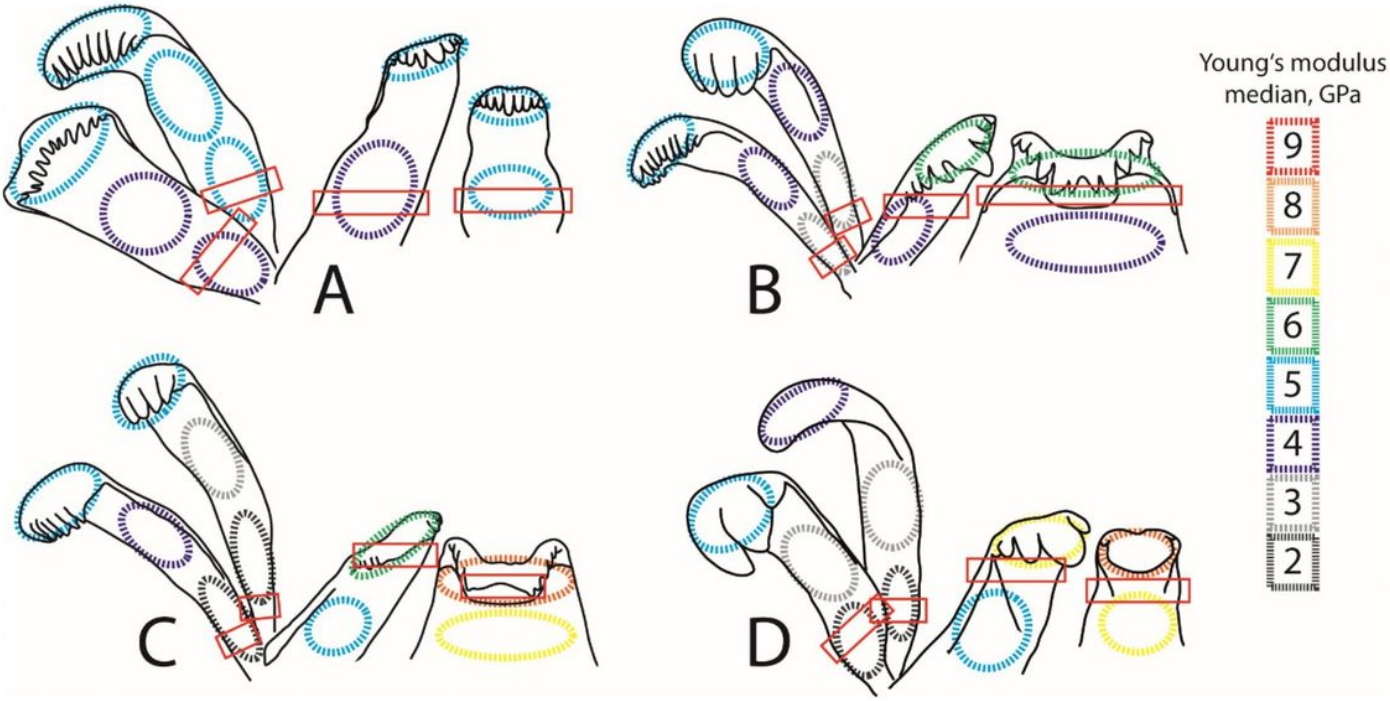

Figure 3

Summary from previous studies on radular teeth failure [84-85]: schematic drawings of radular teeth (adapted from [51]) with median of Young's modulus, in GPa, plotted on the tooth parts (cusp, stylus, basis) for A. Cleopatra johnstoni, B. Bridouxia grandidieriana, C. Spekia zonata, D. Lavigeria grandis. The red boxes highlight the area of failure – if teeth actually broke – during previous breaking stress experiments in wet condition. All marginals broke at their styli close to the basis. In Cleopatra the centrals and laterals also failed at their styli close to the basis. Centrals and laterals in Bridouxia failed between cusps and styli or teeth bended and failed with the adjacent teeth due ripping of the membrane. In Spekia and Lavigeria failure of the centrals and laterals at their denticles or styli was very rarely documented; these teeth rather bended, gained support from adjacent teeth, until all teeth together failed due to rupture of the membrane.

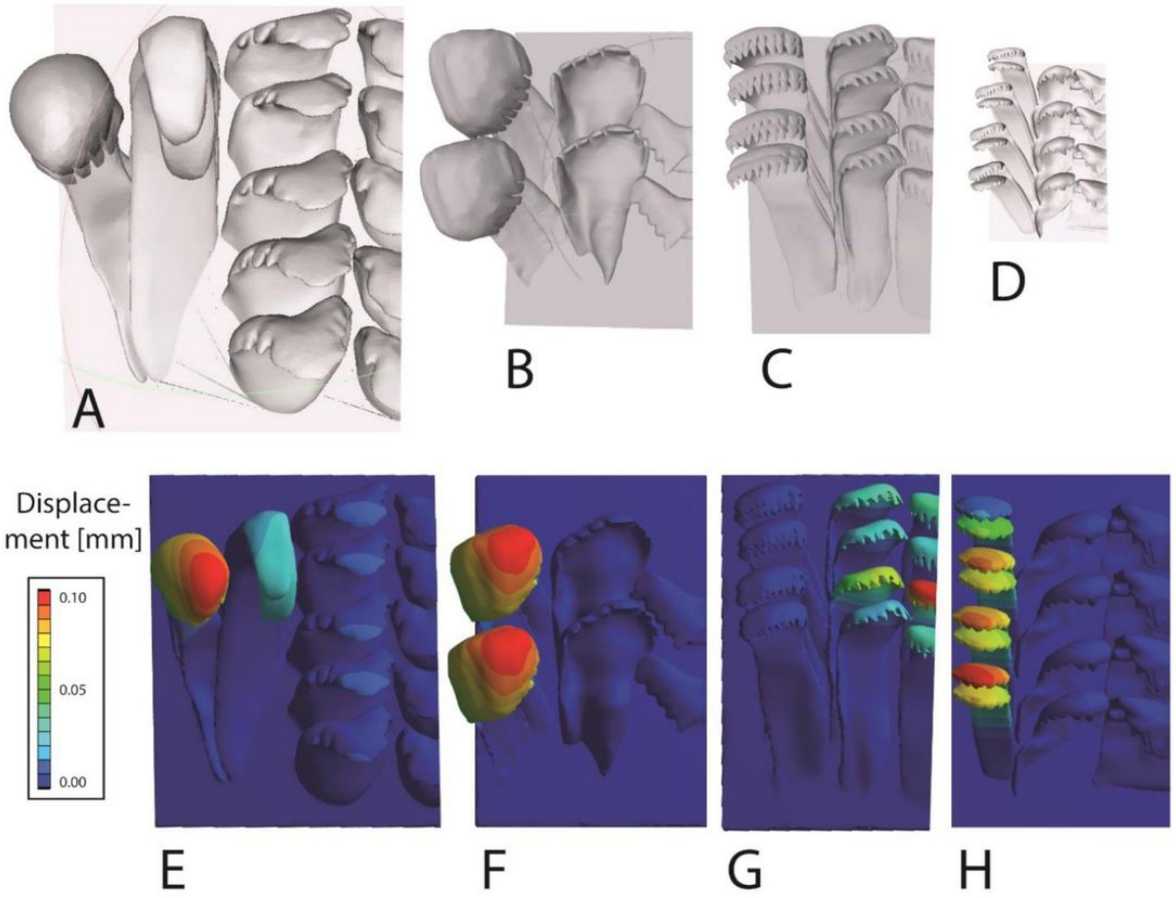

Figure 4

Scaling of the radular teeth as used in the FEA. A,E. Lavigeria, B,F. Spekia, C,G. Cleopatra, D,H. Bridouxia. A–D. Models at the same scale. E–H. Results from the FEA, displacement after being loaded with the nominal force.

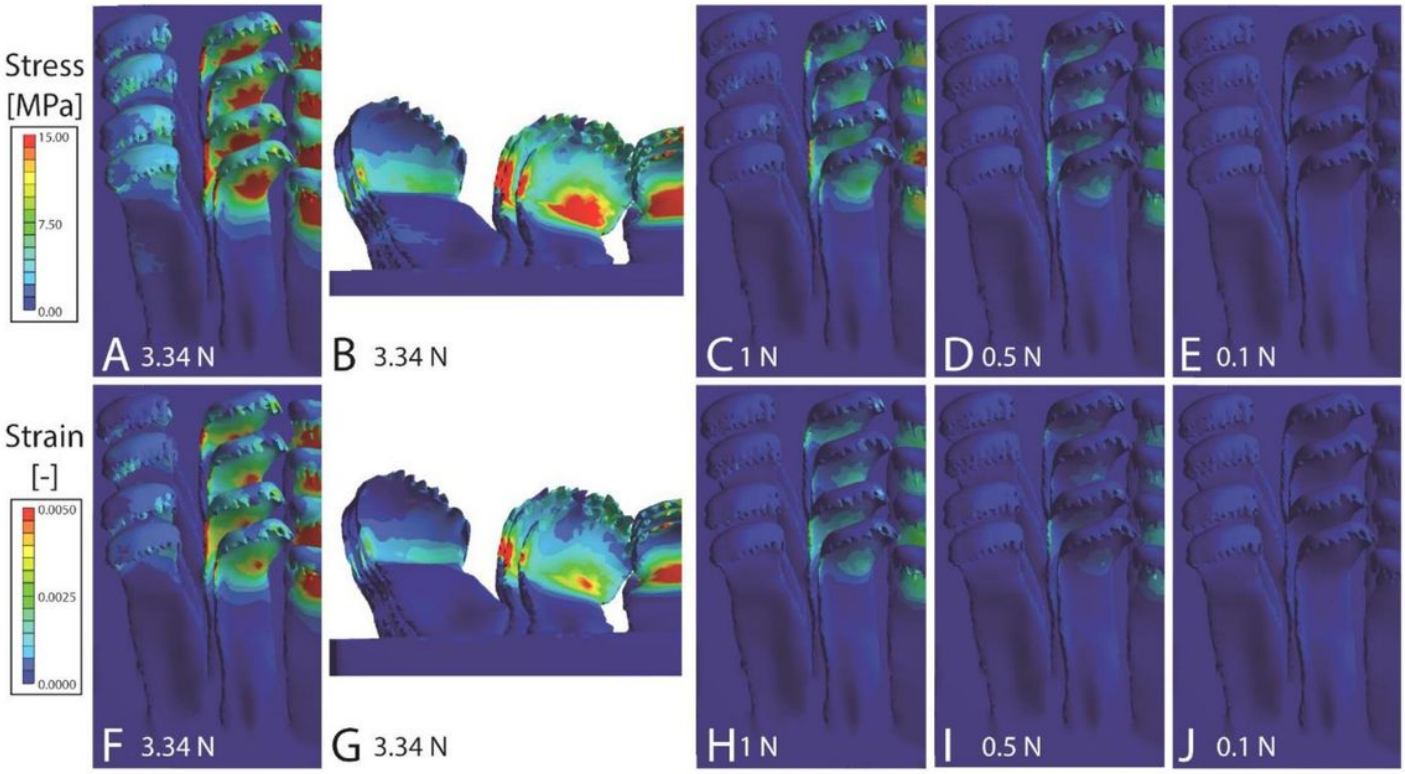

Figure 5

Results from the FEA for Cleopatra. A–E. Stress and F–J. strain. A, B, F, G. Loaded with nominal force (3.34 N); C, H with 1 N; D, I, with 0.5 N; E, J with 0.1 N. The scaling of stress and strain is identical to those in figures 5–8.

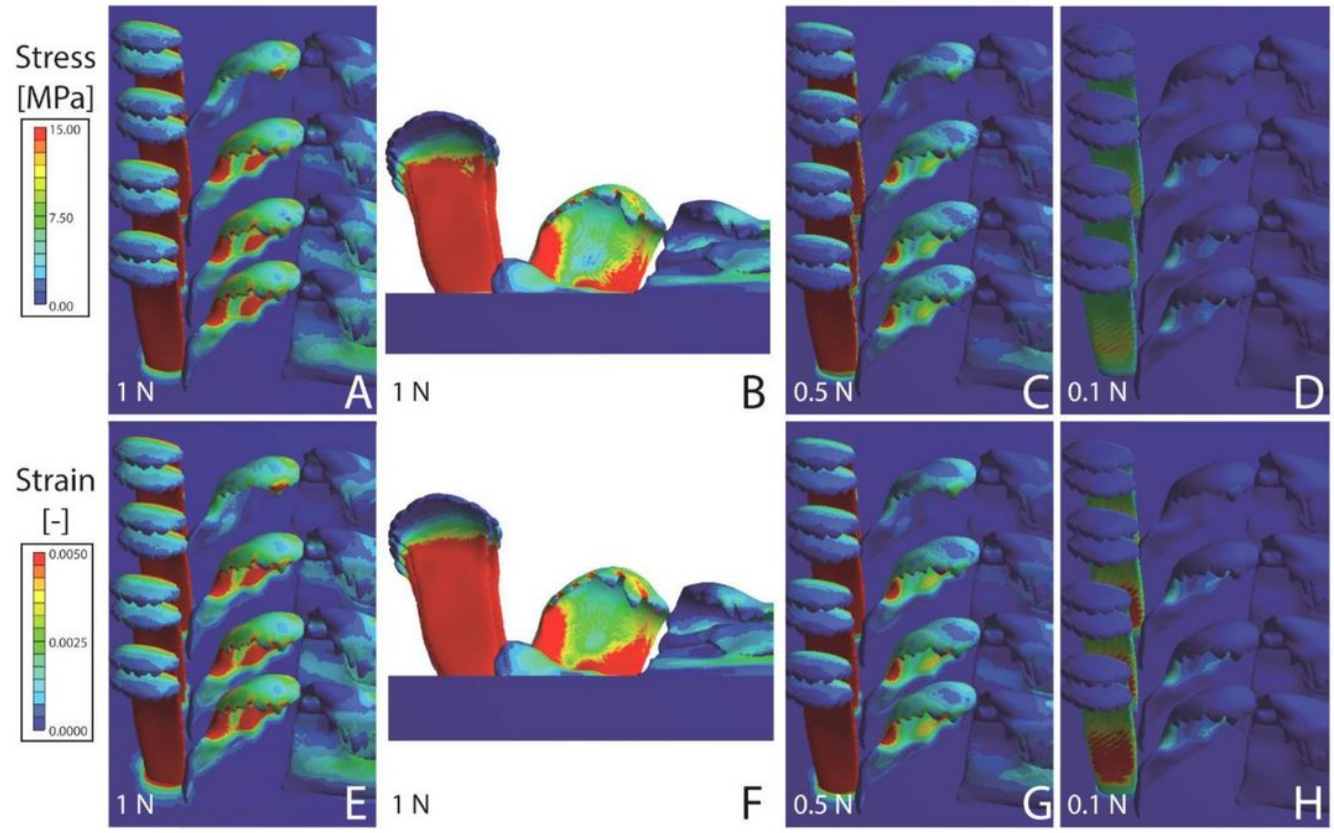

Figure 6

Results from the FEA for Bridouxia. A–E. Stress and F–J. strain. A, B, E, F. Loaded with nominal force (1 N); C, G with 0.5 N; D, H with 0.1 N. The scaling of stress and strain is identical in figures 5–8.

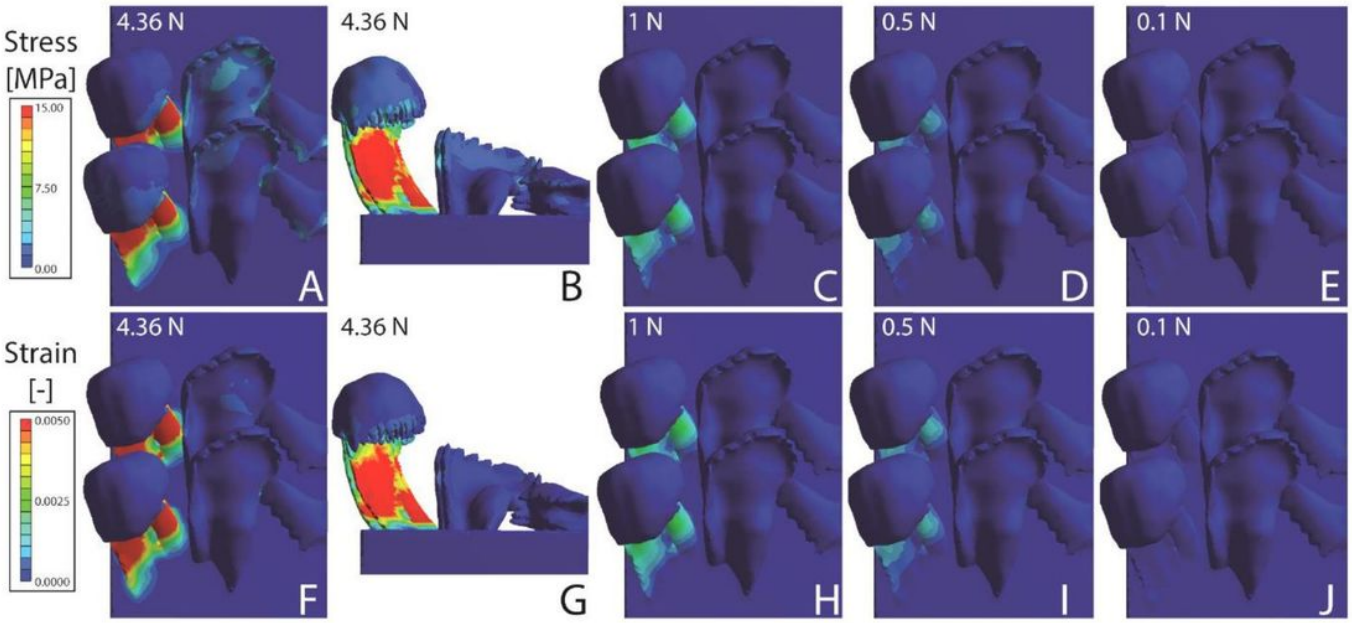

Figure 7

Results from the FEA for Spekia. A–E. Stress and F–J. strain. A, B, F, G. Loaded with nominal force (4.36 N); C, H with 1 N; D, I, with 0.5 N; E, J with 0.1 N. The scaling of stress and strain is identical in figures 5–8.

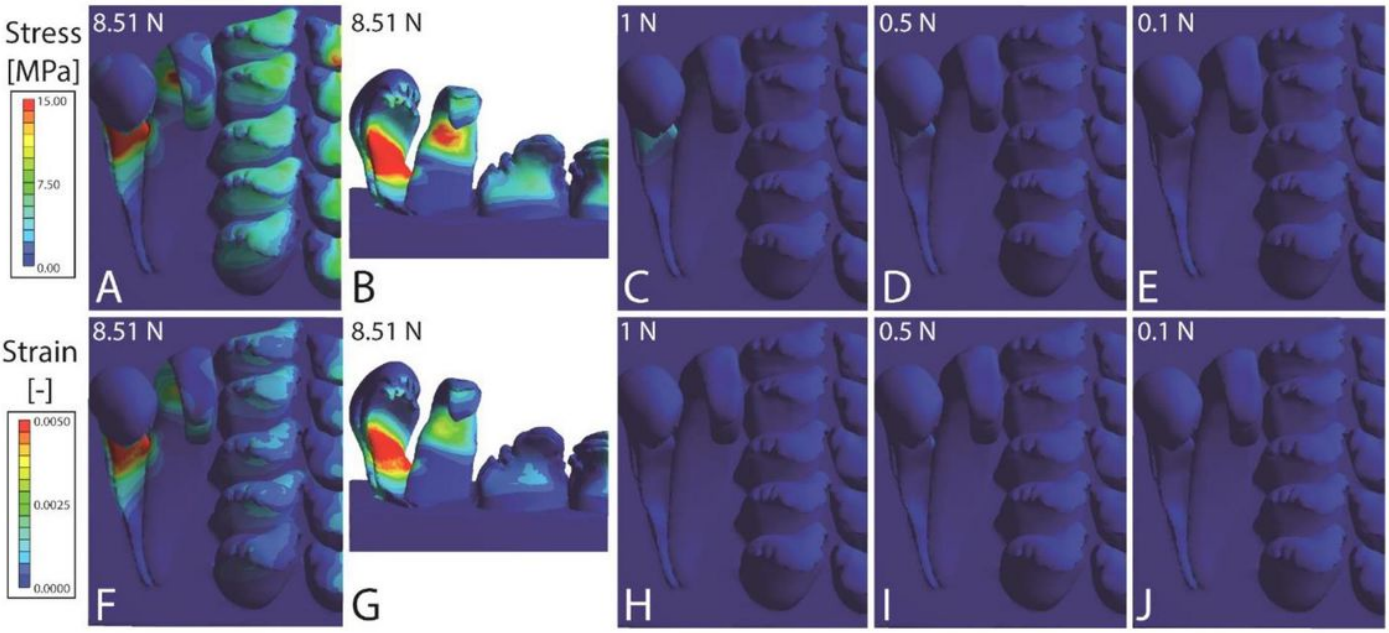

Figure 8

Results from the FEA for Lavigeria. A–E. Stress and F–J. strain. A, B, F, G. Loaded with nominal force (8.51 N); C, H with 1 N; D, I, with 0.5 N; E, J with 0.1 N. The scaling of stress and strain is identical in figures 5–8.